Distortions of polarisation angle in radio pulsars

L. Saha[1], J. Dyks[1], M. Serylak[2], S. Oslowski[3,4], L. Guillemot[5,6], I. Cognard[5,6], and B. Rudak[1]

[1]Nicolaus Copernicus Astronomical Center, Toruń, Poland
[2]Universtity of the Western Cape, Cape Town, South Africa
[3]Fakultät für Physik, Universität Bielefeld, Postfach 100131, 33501 Bielefeld, Germany
[4]Max-Planck-Institut für Radioastronomie, Auf dem Hügel 69, 53121 Bonn, Germany
[5]Laboratoire de Physique et Chimie de l'Environnement et de l'Espace LPC2E
CNRS-Université d'Orléans, F-45071 Orléans, France
[6]Station de radioastronomie de Nançay, Observatoire de Paris, CNRS/INSU F-18330 Nançay, France

February 29, 2016

Abstract

Average profiles of some radio pulsars contain weak emission components which cover large intervals of pulse phase as well as localised emission or absorption features. The polarisation-angle (PA) under such features exhibits local distortions which cannot be explained through the rotating vector model and other effects such as the special relativistic effects or modification of magnetic fields. We show that some of these distortions in the average PA curve can be explained using a simplified physical model of an extended microbeam of the X-mode curvature radiation. Successful interpretation will be presented for features with very different polarisation characteristics, such as the bifurcated emission component on the trailing side of the profile of J0437-4715, and for the double notches observed in B1821-24A and J0437-4715.

1 Introduction

Local distortions of an average curve of PA (ψ) can be found in the PA profiles of many millisecond pulsars, which cannot be explained using simple rotating vector model (RVM). Here we study a model which assumes an extended microbeam of the extraordinary polarisation mode (X-mode) curvature radiation (CR) polarised at a fixed position angle within an interval of pulse phase. We use this model to explain observed local PA distortions for two millisecond pulsars: PSR B1821−24A (Nançay data, Fig. 1a-d) and PSR J0437−4715 (Parkes data from Dai et al. 2015, Fig. 1e-h; cf. Oslowski et al. 2014).

Bifurcated features in the profiles of these objects are coincident with interesting polarisation effects. At the pulse phase $\phi \approx 100^\circ$ the profile of PSR B1821-24A contains double notches which are coincident with a sharp drop of linear polarisation fraction ($\Pi = L/I$, grey line in Fig. 1c), and with a sudden change of polarisation angle (ψ) by about 15° (dots in Fig. 1d; for a view with higher S/N – see Fig. 2 in Bilous et al. 2015). The profile of PSR J0437-4715 also contains double notches (at $\phi \approx 69^\circ$) albeit with a different polarisation properties. The PA deflects there in a 'W'-shaped way (Fig. 1h, dots), and the polarisation fraction drops down by just 25 per cent (Fig. 1g, grey line).

2 Model and discussion

The model assumes that the radio emission is coming from a plasma stream following a narrow magnetic flux tube, with no radiation emitted strictly within the plane of the electron trajectory (see Fig. 1 of Ref. [3]). The process of CR in the X-mode or ⊥-mode provides an example of such a double-lobed beam (or fan-beam). In the case of emission in vacuum, the CR beam can be mathematically

decomposed into two parts: a filled-in pencil beam polarised in the plane of the B-field lines and the bifurcated beam polarised at the right angle to the plane of B. The strongly-magnetised plasma splits the beam into two modes: the filled-in part polarised parallel to the B-field line plane (O mode) and the bifurcated X-mode part. The net polarisation of the X-mode beam, i.e. the polarisation recorded after the beam has fully swept across our line of sight, is orthogonal to the plane of the B-field line [4, 5, 10]. Fig. 2a shows a sky-projected view of such a double-lobed beam. Each point on the stream (say the point 'a' in Fig. 2a) creates two bright patches of quasi-instantaneous emission on the sky (a_L and a_T). Continuous motion of charges then gives rise to a split fan beam, which, when crossed by the line of sight, is perceived as a bifurcated emission component. The bifurcated features observed in "absorption" (double notches), are produced by another arrangement of emission region: a laterally-extended region is emitting the bifurcated microbeams. A narrow plasma stream is either non-emitting and immersed in the emitter, or the stream is located above the emitter, and obscures the latter. The passage of sightline through such a stream gives rise to the double notches observed in the data. The key assumption of our model, consistent with the properties of CR, is that the fixed value of PA, which corresponds to the guiding magnetic field line (Ψ_B in Fig. 2a), is contributed within a wide interval of pulse phase, subtending the lobes a_L and b_T in Fig. 2a.

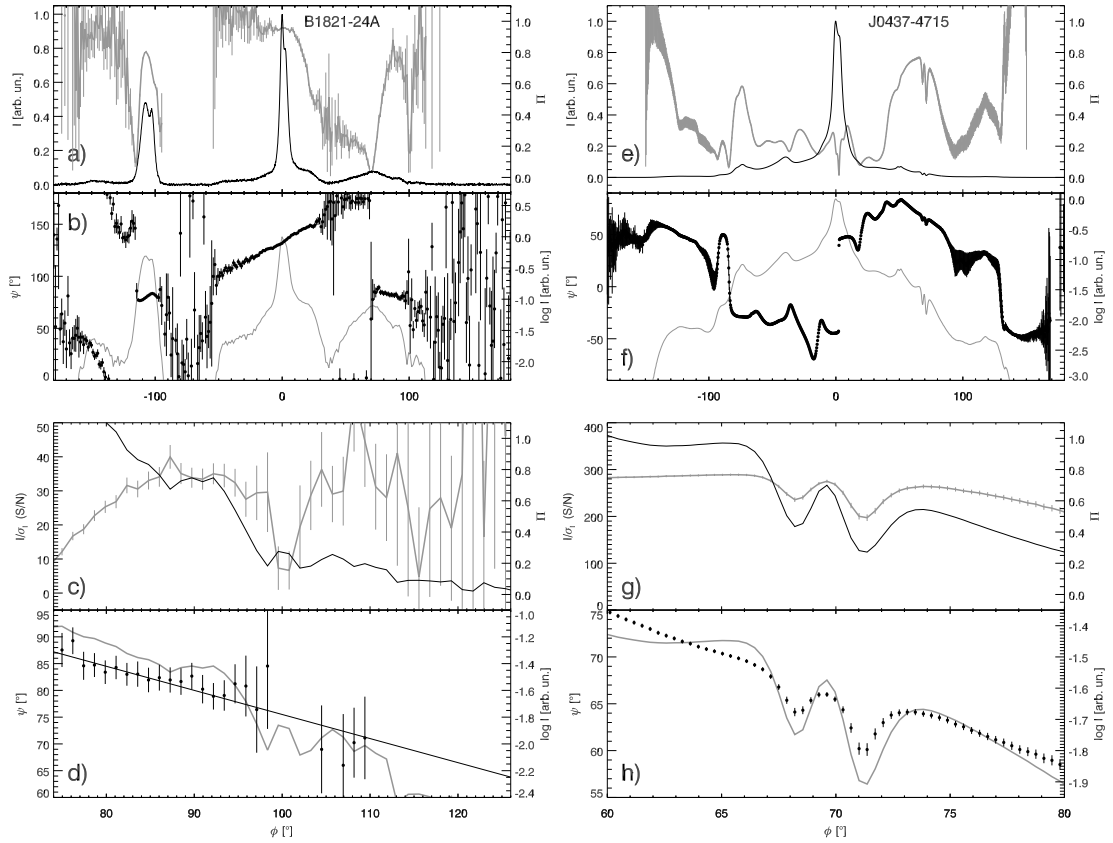

Figure 1: Linear polarization properties of PSR B1821-24A (left) and PSR J0437-4715 (right) as observed in L band with Nançay and Parkes telescope, respectively. **a)** Total flux I (black solid) and the linear polarisation fraction $\Pi = L/I$ (grey). **b)** The PA (black) and $\log I$ (grey). **c)** The total flux S/N (black solid) and the polarisation fraction (grey). **d)** The PA (black) and $\log I$ (grey). The straight line presents the PA variations anticipated in the absence of the notches. Note the drop of Π and the change of PA at the notches. Data for J0437−4715 are from Dai et al. (2015).

To model the polarisation profile we assume a lateral profile (analytical function $\eta_\perp$) for the macroscopic emissivity probed by our line of sight. A single void or peak in $\eta_\perp$ is considered to cause double notches or bifurcated components in the pulse profile. In the calculation shown in panels b and c of Fig. 2, the microbeam pattern of the pure X-mode CR (dot-dashed line in Fig. 2b) is convolved with the macroscopic emissivity profile ($\eta_\perp$, thick solid in Fig. 2b) to produce the net intensity profile $I_\perp$ (thin solid line in 2b). The calculated net PA is shown in Fig. 2c with a solid near-diagonal line.

The grey split stripe presents the distribution of intrinsic PA values, which contribute to the average. The stripe is broken at phase 'D', because of the Gaussian void in the spatial emissivity profile $\eta_\perp$. A vertical (fixed-phase) average of the intrinsic PA at the phase marked with 'C', leads to the upward deflection of the net PA, because the flux at C is dominated by emission from phase B, with a larger PA. For similar reason, on the right-hand side of D, the net PA deflects downwards by the same magnitude. This creates a zigzag-shaped wiggle of the net PA (the solid near-diagonal line) around the reference PA, which is assumed to represent the traditional RVM (ψ_B, marked with dotted line). This behaviour is observed within the notches of PSR B1821−24A (Fig. 1d; cf. Fig. 2 in Bilous et al. 2015).

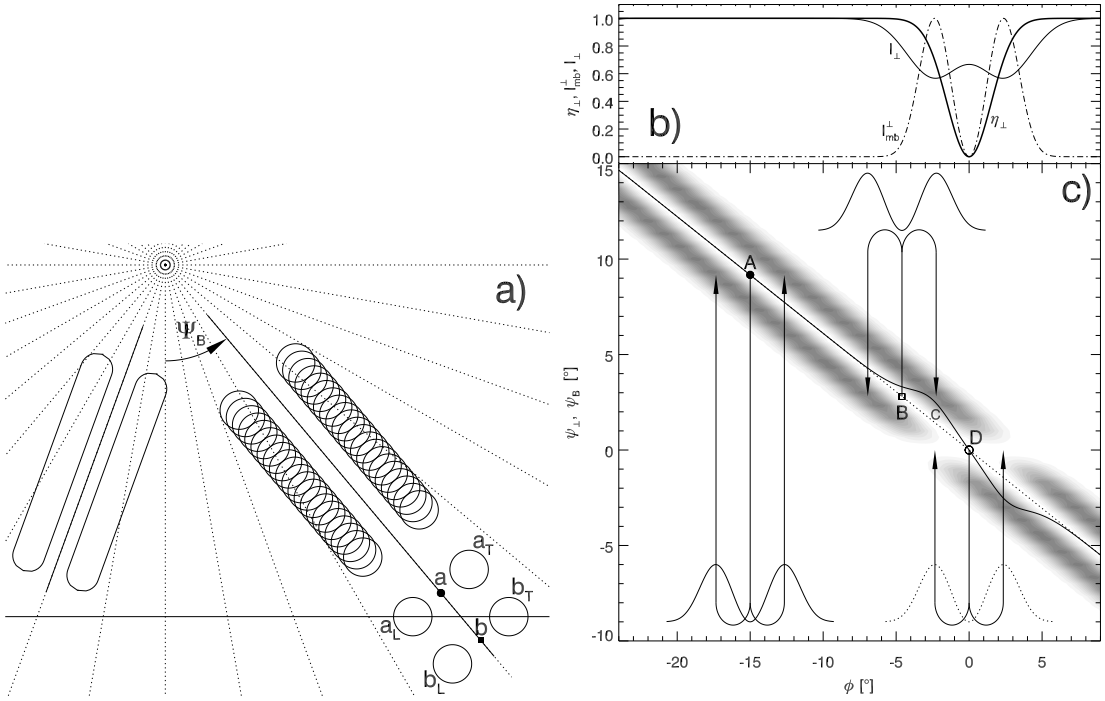

Figure 2: a) A sky-projected view of the split-fan beams typical of the X-mode curvature radiation from narrow plasma streams. b) The mechanism of the bidirectional (zigzag-shaped) PA distortion. The effective microbeam pattern, I_{mb} (dashed), the macroscopic X-mode emissivity profile $\eta_\perp$ (thick solid) and net intensity profile $I_\perp$ (thin solid). c) The PA as a function of phase. PA distribution for bifurcated microbeam is shown with grey-scale plot. The near-diagonal solid line marks $\psi_\perp$, i.e. the net value of the X-mode PA. Dotted line marks the RVM-based reference (ψ_B). The double-peaked microbeams, with arrows emerging from points A and B, present how the PA is distributed within the neighbouring pulse longitudes.

In the case of PSR J0437−4715 (Fig. 1h), the PA at both minima in the notches deflects in the same direction (downward). This behaviour can be reproduced by adding a moderate contribution of radiation in the other quasi-orthogonal polarisation mode (O mode). Fig. 3 presents the model result for a rectangular void in the X-mode emissivity profile (thick solid in Fig. 3a) with a uniform contribution of O mode (dashed line in Fig. 3b), polarised at the angle of 60° with respect to the reference PA. The presence of the other, not precisely orthogonal mode, transforms the zigzag deflection into a 'W'-shaped distortion (Fig. 3d, thick solid). At the same time, the model qualitatively reproduces the total intensity (I, thick solid in Fig. 3c) and the polarisation fraction (thin solid in 3c). In a full version of this paper (Dyks et al. 2016, MNRAS, submitted) it is shown that with this type of a model one can also interpret the PA distortion observed at the trailing bifurcated emission component present in the profile of J0437−4715.

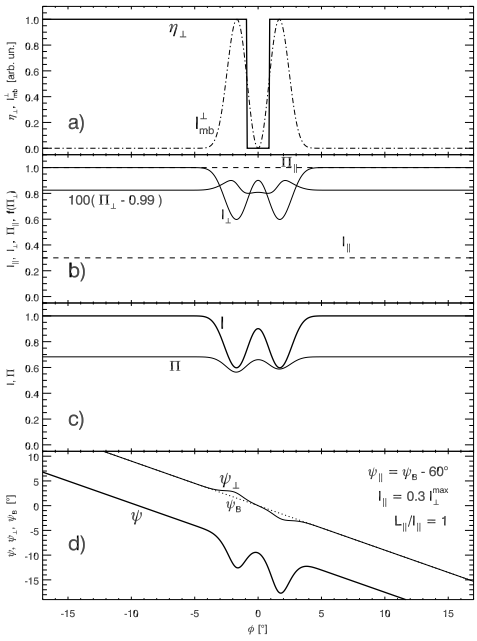

Figure 3: Model results which reproduce the observed properties of the double notches in PSR J0437–4715 (see Fig. 1g,h). a) Thick solid line: a rectangular void in emissivity, of a half-width equal to 0.9°. b) Intensity and polarisation fraction for both modes (⊥-mode: solid; ∥-mode: dashed). $\Pi_\perp$ is indiscernible from $\Pi_\parallel = 1$, hence we plot $100(\Pi_\perp - 0.99)$. c) Total intensity (thick solid) and the total Π (thin). d) The total PA ψ is shown with thick solid line. The X-mode PA ($\psi_\perp$, thin solid) is shown separately with the reference ψ_B of the RVM model (dotted).

3 Conclusion

The PA distortions observed at localised double features in radio pulsar profiles can be understood with a model which assumes that the elementary emission region in pulsar magnetosphere has the shape of a narrow but long plasma stream. The stream is locally emitting a bifurcated, a few degrees wide, beam of radiation, which gives rise to a fan beam. Such a fan beam contributes a fixed value of PA, as determined by the stream's central magnetic field line, within an interval of pulse phase. The success of such a model in reproducing the polarisation behaviour of several dissimilar PA features in PSR B1821-24A and J0437-4715 provides additional support for the stream-shaped geometry of pulsar emission region, as well as for the fan-shaped geometry of pulsar beams [3, 6, 7, 9]. It also shows that the CR is a useful mechanism for interpreting the pulsar radio emission.

Acknowledgment

This work has been funded by the National Science Center (Poland), within the project DEC-2011/02/A/ST9/00256.

References

[1] Bilous, A. V., Pennucci, T. T., Demorest, P., Ransom, S. M., 2015, ApJ, 803, 83

[2] Dai, S., Hobbs, G., Manchester, R. N., et al., 2015, MNRAS, 449, 3223

[3] Dyks, J., Rudak, B., 2012, MNRAS, 420, 3403

[4] Lyubarsky Y., 2008, 40 Years of Pulsars: Millisecond Pulsars, Magnetars and More, Vol. 983 of American Institute of Physics Conference Series, Pulsar emission mechanisms

[5] Gil, J., Lyubarsky, Y., Melikidze, G. I., 2004, ApJ, 600, 872

[6] Dyks, J., Rudak, B., 2015, MNRAS, 446, 2505

[7] Michel, F. C., 1987, ApJ, 322, 822

[8] Oslowski S., van Straten W., Bailes M., Jameson A., Hobbs G., 2014, MNRAS, 441, 3148

[9] Wang, H. G., Pi, F. P., Zheng, X. P., et al., 2014, ApJ, 789, 73

[10] Wang, P. F., Wang, C., & Han, J. L., 2014, MNRAS, 441, 1943